

# Design and Performance Improvement of Three-Dimensional Optical Code Division Multiple Access Networks with NAND Detection Technique

Satyasen Panda, Urmila Bhanja

**Abstract**—In this paper, we have presented and analyzed three-dimensional (3-D) matrices of wavelength/time/space code for optical code division multiple access (OCDMA) networks with NAND subtraction detection technique. The 3-D codes are constructed by integrating a two-dimensional modified quadratic congruence (MQC) code with one-dimensional modified prime (MP) code. The respective encoders and decoders were designed using fiber Bragg gratings and optical delay lines to minimize the bit error rate (BER). The performance analysis of the 3D-OCDMA system is based on measurement of signal to noise ratio (SNR), BER and eye diagram for a different number of simultaneous users. Also, in the analysis, various types of noises and multiple access interference (MAI) effects were considered. The results obtained with NAND detection technique were compared with those obtained with OR and AND subtraction techniques. The comparison results proved that the NAND detection technique with 3-D MQC/MP code can accommodate more number of simultaneous users for longer distances of fiber with minimum BER as compared to OR and AND subtraction techniques. The received optical power is also measured at various levels of BER to analyze the effect of attenuation.

**Keywords**—Cross correlation, three-dimensional optical code division multiple access, spectral amplitude coding optical code division multiple access, multiple access interference, phase induced intensity noise, three-dimensional modified quadratic congruence/modified prime code.

## I. INTRODUCTION

THE optical CDMA technique is one of the most advanced techniques in recent times for optical access networks which support large number of active users by using available frequency with less time delay, providing flexible provisioning, higher data rate transmission, lower BER and security [1]. But the OCDMA systems always suffer due to the influence of various types of noises like thermal noise, shot noise, phase induced intensity noise (PIIN) and most importantly MAI [2]. In OCDMA systems, different types of codes have been proposed like one-dimensional (1-D) codes, which spread in time or frequency, and two-dimensional (2-D) codes, which spread in both time and wavelength. With the increase in number of active users in the OCDMA network, the MAI increases degrading system performance. To minimize MAI, the number of chip collisions in the receiver should be less, the length of the code should be increased and

the weight of the code chips should be reduced. By increasing the length of the one-dimensional unipolar code and two dimensional codes, the complexity of the encoder and decoder increases which reduces the data transmission rate. To nullify the above system limitations, we have constructed 3-D OCDMA code (MQC/MP) by combining 2-D MQC code [3] and 1-D MP code [4]. In 3-D OCDMA coding, pulses are placed in various chips of different wavelength across the bit period, making a wavelength hopping pattern which performs increased code design flexibility and better coding performance. Here all simultaneous users share the exact wavelength, time domain and space achieving better division of wavelength, synchronous access and easier network control and management.

To improve the system performance of OCDMA systems by decreasing MAI, various detection mechanisms have been adopted by modifying designs of transmitters and receivers. The basic detection techniques are coherent detection techniques and incoherent detection techniques. Coherent detection techniques are executed in a bipolar behavior with the coding operation and also have the knowledge of phase information of the carrier while sending the detection signal, but it requires phase synchronizations and complex hardware. However, the incoherent detection technique does not require phase synchronization, complex hardware and it is performed in a unipolar environment to improve the system performance. There are various types of incoherent detection techniques like complementary subtraction technique, AND subtraction technique [5], spectral detection technique (SDD) [6] and OR detection technique. These detection techniques can minimize MAI but the performance degrades due to poor signal quality. Taking into account these limitations of the MQC/MP 3-D code with AND, OR and SDD detection techniques, we devised NAND subtraction detection [7] for this analysis to improve system performance. We have analyzed the overall system performance by mathematical analysis and simulation analysis to obtain results by experimenting MQC/MP 3-D code with the NAND detection technique, which is compared with those as obtained by AND and OR detection techniques. The comparison results proved that the system performance improved a lot by using MQC/MP code with NAND detection technique compared to other detection techniques in terms of better signal quality and easier implementation.

The remaining paper is organized as follows. Section II provides the construction mechanism of MQC/MP 3-D OCDMA code. Section III shows the procedures of NAND

Satyasen Panda, PhD Scholar, and Dr. Urmila Bhanja, Associate Professor, are with the Department of Electronics and Communication Engineering, IGIT, Sarang, India (e-mail: satyasenp@gmail.com, urmilabhanja@gmail.com).

detection technique. The system performance analysis is provided in Section IV. In Section V, network simulation set up has been presented. Section VI contains the discussion on simulation results. Finally, conclusions are drawn in Section VII.

TABLE I  
 MQC CODE SEQUENCE FOR P=5

| $i$ | $j$ | $t_{i,j}(k)$ | $x(l)$ |       |       |     |
|-----|-----|--------------|--------|-------|-------|-----|
| 0   | 0   | 014412       | 10000  | 01000 | 00001 | 000 |
|     |     |              | 01     | 01000 | 00100 |     |
| 1   | 0   | 144103       | 01000  | 00001 | 00001 | 010 |
|     |     |              | 00     | 10000 | 00010 |     |
| 4   | 0   | 101441       | 01000  | 10000 | 01000 | 000 |
|     |     |              | 01     | 01000 | 01000 |     |
| 1   | 3   | 422433       | 00001  | 00100 | 00100 | 000 |
|     |     |              | 01     | 00010 | 00010 |     |
| 3   | 4   | 304030       | 00010  | 10000 | 00001 | 100 |
|     |     |              | 00     | 00010 | 10000 |     |

### II. 3-D MQC/MP CODE CONSTRUCTION

The 3-D MQC/MP code is constructed by combining the features of wavelength hopping and temporal spreading MQC codes and Spatial coded MP codes. The 3-D MQC/MP code with  $X$  as number of wavelengths,  $Y$  as the temporal code length and  $Z$  as the spatial code length,  $W$  as weight,  $\lambda_a$  and  $\lambda_c$  are auto correlation and cross correlation values referred as  $(X \times Y \times Z, W, \lambda_a, \lambda_c)$ .

The following steps describe the construction of 2-D MQC/MP code for various orders.

#### A. MQC Code Construction

The MQC codes can be constructed using the following stages.

**Stage 1.** In this stage, we first have to construct a sequence of integer numbers as  $t_{i,j}(k)$  that are elements of a Galois finite field  $GF(p)$  over an odd prime  $p$  ( $p > 2$ ) using:

$$t_{i,j}(k) = \begin{cases} [c(k+i)^2 + j] \pmod{p}, & k = 0, 1, \dots, p-1 \\ [i+b] \pmod{p}, & k = p \end{cases} \quad (1)$$

where  $c \in \{1, 2, \dots, p-1\}$  and  $b, i, j \in \{0, 1, 2, \dots, p-1\}$ .

Every sequence  $t_{i,j}(k)$  has  $p+1$  elements and  $p^2$  different code sequences for every pair of parameters  $c$  and  $b$  by modifying parameters  $i$  and  $j$  to generate  $p(p-1)$  code families.

**Stage 2.** To construct a sequence of binary numbers (0, 1) as  $x(l)$  based on original sequence  $t_{i,j}(k)$ , the following mapping method is used:

$$x_{i,j}(l) = \begin{cases} 1 & \text{if } l = kp + t_{i,j}(k) \\ 0 & \text{otherwise} \end{cases} \quad (2)$$

where  $l = 0, 1, 2, 3, \dots, p^2 - 1$  and  $k = \left\lfloor \frac{l}{p} \right\rfloor$  representing highest number less than or equal to the value of  $(l/p)$ .

The following MQC code sequences can be generated by using the parameters  $p=5, c=1$  and  $b=2$ , as shown in Table I.

Each of the MQC code sequences contains  $p^2 + p$  elements that can be subdivided into  $p+1$  groups where each group contains one "1" and  $(p-1)$  "0"s.

#### B. MP Code Construction

The MP codes can be constructed using the following stages.

**Stage 1.** The construction of MP code starts with considering Galois field  $GF(p)$  of a prime number  $p$ . A MP sequence  $y_{\alpha,\beta}(z)$  can be designed by taking elements of Galois field with an odd prime number using:

$$y_{\alpha,\beta}(z) = \begin{cases} (\alpha + \beta z) \odot p, & z = 0, 1, 2, \dots, p-1 \\ \beta, & z = p \end{cases} \quad (3)$$

where  $\alpha \in \{0, 1, 2, \dots, p-1\}$  and  $\beta \in \{0, 1, 2, \dots, p-1\}$ .

By using (3), a prime code family of  $p^2$  sequences can be generated for different values of parameters  $\alpha$  and  $\beta$ . A prime code set of PC for  $p=5$  is established by Table II.

TABLE II  
 A PRIME CODE SET OF PC FOR P=5

|        |   |   |   |   |   |
|--------|---|---|---|---|---|
| $y(0)$ | 0 | 0 | 0 | 0 | 0 |
| $y(1)$ | 0 | 1 | 2 | 3 | 4 |
| $y(2)$ | 0 | 2 | 4 | 1 | 3 |
| $y(3)$ | 0 | 3 | 1 | 4 | 2 |
| $y(4)$ | 0 | 4 | 3 | 2 | 1 |

Considering each number in the above code set in Table I consisting of  $p$  time slots, the value of the no plus '1' is the location of the optical pulse. Thus, Table I can be modified to get the prime code (PC), as shown in Table III.

TABLE III  
 A PRIME CODE SET OF PC FOR P=5

|        |   |   |   |   |   |
|--------|---|---|---|---|---|
| $y(0)$ | 1 | 1 | 1 | 1 | 1 |
| $y(1)$ | 1 | 2 | 3 | 4 | 5 |
| $y(2)$ | 1 | 3 | 5 | 2 | 4 |
| $y(3)$ | 1 | 4 | 2 | 5 | 3 |
| $y(4)$ | 1 | 5 | 4 | 3 | 2 |

**Stage 2.** To generate a MP code from the prime code sequence, each sequence is mapped into a binary form (0, 1). The MP code sequence will be:

$$y_\gamma = \{d_\gamma(0), d_\gamma(1), d_\gamma(2), \dots, d_\gamma(p^2 + p - 1)\} \quad (4)$$

where

$$d_\gamma(s) = \begin{cases} 1, & \text{where } s = zp + y_{\alpha,\beta}(z) \\ 0, & \text{otherwise} \end{cases} \quad (5)$$

Here  $s = 0, 1, 2, \dots, p^2 + p - 1$  and  $\gamma = 0, 1, \dots, p^2 - 1$ . Here each  $\gamma$  represents the position of '1' in a string of 5 bits where other four bits are '0'. The prime code has a correlation of one, as represented in Table IV.

TABLE IV  
 A MP CODE SET OF MPC FOR P=5

|        |       |       |       |       |       |
|--------|-------|-------|-------|-------|-------|
| $D(0)$ | 10000 | 10000 | 10000 | 10000 | 10000 |
| $D(1)$ | 10000 | 01000 | 00100 | 00010 | 00001 |
| $D(3)$ | 10000 | 00100 | 00001 | 01000 | 00010 |
| $D(4)$ | 10000 | 00010 | 01000 | 00001 | 00100 |
| $D(5)$ | 10000 | 00001 | 00010 | 00100 | 01000 |

### C. MQC/MP Code Construction

The 3-D MQC/MP code matrices can be generated using:

$$m_{i,j,\gamma} = \begin{bmatrix} d_\gamma(0)x_{i,j}(l) \\ d_\gamma(1)x_{i,j}(l) \\ d_\gamma(2)x_{i,j}(l) \\ \vdots \\ d_\gamma(p^2 + p - 1)x_{i,j}(l) \end{bmatrix} \quad (6)$$

where  $l = 0, 1, 2, 3, \dots, p^2 - 1$  and  $\gamma \in \{0, 1, 2, \dots, p^2 - 1\}$ .

### III. NAND SUBTRACTION TECHNIQUE

In digital electronics NAND gate performs the complementary operation of AND gate. In our proposed analysis, the concept of NAND is used as an operation for NAND subtraction detection technique to improve the system performance in the receiver side because the mobility of electrons inside NAND gate is three times greater than AND, OR and NOR gates. In this technique, the cross-correlation  $\varphi_{(\overline{AB})}(k)$  represents NAND operation between A and B sequence. If we take  $A=1\ 0\ 1\ 0$  and  $B=1\ 1\ 0\ 0$ , then NAND of A and B is  $(\overline{AB})=0\ 1\ 1\ 1$ . Since NAND subtraction technique identifies similar spectral position of chips in a much better way, the code weight is increased which further increases Signal power and Signal-to-Noise ratio (SNR). So the OCDMA system performance is highly improved by using the NAND subtraction technique. Table V provides the comparison between NAND, AND and OR subtraction technique.

TABLE V  
 COMPARISON BETWEEN NAND, AND & OR SUBTRACTION TECHNIQUE

| Spectral position | A | B | OR | AND | NAND |
|-------------------|---|---|----|-----|------|
| S1                | 1 | 1 | 0  | 1   | 0    |
| S2                | 0 | 1 | 1  | 0   | 1    |
| S3                | 1 | 0 | 1  | 0   | 1    |
| S4                | 0 | 0 | 0  | 0   | 1    |

### IV. SYSTEM PERFORMANCE ANALYSIS

For the analysis of our system, Gaussian approximation is used for the calculation of BER. Since 3-D MQC/MP code has

zero to one cross-correlation property, there is no overlapping in the spectra of different users, which reduces the MAI improving the overall system performance. In this paper, for 3-D MQC/MP code, thermal noise ( $\sigma_t$ ), PIIN and shot noise ( $\sigma_{sh}$ ) in the photo detectors are considered. The performance of an optical receiver depends on the SNR. The SNR of an electrical signal is defined as the average signal power to noise power ( $SNR = \frac{I^2}{\sigma^2}$ ), where  $\sigma^2$  is defined as the variance of different noise sources.  $I$  is the average photo current and  $I^2$  is the aggregate signal power

For MQC/MP code, the composite noise variance [8] can be:

$$\sigma^2 = \sigma_{shot}^2 + \sigma_t^2 + \sigma_{PIIN}^2 = 2eI_{shot}B + \frac{4K_B T_n B}{R_L} + I_{PIIN}^2 B t_c \quad (7)$$

where 'e' is the electronic charge is the noise equivalent of electrical bandwidth of the receiver,  $K_B$  is Boltzmann's constant,  $T_n$  is the absolute receiver temperature,  $t_c$  is coherent time of light incident to photo diode,  $R_L$  is the receiver load resistance,  $I_{shot}$  is the shot noise current and  $I_{PIIN}$  is the PIIN noise current.

The  $i$ -th user of 3D MQC/MP code  $C_{i,j,q}^k$  is a matrix of M row vectors and  $b_{N,S}^k$  is related to temporal/Spatial spreading.

$$b_{1,N,S}^k = [c_{\lambda,1,1}^k, c_{\lambda,2,2}^k, \dots, c_{\lambda,N,S}^k] \quad (8)$$

where  $c_{\lambda,N,S}^k \in \{1, 0\}$ .

Here emitted wavelengths of  $\lambda \in \{1, 2, \dots, M\}$ .

$$c_{i,j,q}^k = \begin{bmatrix} b_{1,1,1}^k \\ b_{2,2,2}^k \\ \vdots \\ b_{M,N,S}^k \end{bmatrix} \quad (9)$$

The 3-D MQC/MP code cross correlation using NAND detection technique is much lower than other detection techniques. Since this technique provides better system performance by reducing PIIN noise, shot noise, signal-to-noise ratio (SNR) and bit-error-rate (BER), it has become the most preferred detection technique. This NAND detection technique on MQC/MP 3-D code is described in:

$$\sum_{i=1}^M \overline{(c_{i,j,q}^k c_{i,j,q}^l)} c_{i,j,q}^l = \begin{cases} W & \text{for } k=l \\ W-1 & \text{for } k \neq l \\ 0 & \text{otherwise} \end{cases} \quad (10)$$

Since shot noise, PIIN and thermal noise obey negative binomial distribution, the following assumptions are used to analyze the system with transmitter and receiver without much difficulty and for mathematical straightforwardness. The assumptions [9] are:

- Each light source is ideally un-polarized and its spectrum is flat over the bandwidth  $[v_0 - \Delta v/2, v_0 + \Delta v/2]$ , where  $v_0$  the central optical frequency is and  $\Delta v$  is the optical source bandwidth expressed in Hz.
- Each power spectral component has equivalent spectral width.
- Each user has equal power at the receiver.
- Bit streams from different transmitters are synchronized
- The effect of PIIN, Shot Noise and Thermal Noise obey Gaussian distribution.

Using the above assumptions, the system performance is analyzed using Gaussian approximation. The Power Spectral density (PSD) of the received optical signal is described [10] as:

$$r(v) = \frac{P_r}{\Delta v k_s} \sum_{k=1}^k b_k \sum_{i=1}^M \sum_{j=1}^N \sum_{q=1}^S c_{i,j,q}(w) \text{rect}(v, i) \quad (11)$$

$P_r$  is the effective power of a broadband source at the receiver,  $c_{i,j}(w)$  is the element of  $w$ -th user's codeword,  $k$  is the no of active users,  $M$  is the spectral code sequence code length,  $N$  is the temporal code sequence code length,  $k_s$  is the spatial code sequence code weight,  $b_k$  is the data bit of the  $k$ -th user.

The  $\text{rect}(v, i)$  function is given by:

$$\text{rect}(v, i) = \left[ v - v_0 - \frac{\Delta v}{2M}(-M+2i) \right] - u \left[ v - v_0 - \frac{\Delta v}{2M}(-M+2i-2) \right] \quad (12)$$

where  $u(v)$  represents unit step function.

The aggregate power spectral density at the input of photo detector one (PD1) in Fig. 3 is given by:

$$\begin{aligned} P_1 &= \int_0^\infty G_1(v) dv = \\ &= \int_0^\infty \left[ \frac{P_r}{\Delta v k_s} \sum_{k=1}^k b_k \sum_{i=1}^M \sum_{j=1}^N \sum_{q=1}^S c_{i,j,q}^k(w) c_{i,j,q}^l(w) \text{rect}(v, i) \right] dv \quad (13) \\ &= \frac{P_r}{MN-1} \sum_{k=1}^k b_k \end{aligned}$$

The Power spectral density at the input of photo detector two (PD2) in Fig. 3 is given by:

$$\begin{aligned} P_2 &= \int_0^\infty G_2(v) dv = \\ &= \int_0^\infty \left[ \frac{P_r}{\Delta v k_s} \sum_{k=1}^k b_k \sum_{i=1}^M \sum_{j=1}^N \sum_{q=1}^S \overline{(c_{i,j,q}^k(w) c_{i,j,q}^l(w))} c_{i,j,q}^k(w) \text{rect}(v, i) \right] dv \quad (14) \\ &= \frac{P_r}{MN-1} [W + (W-1) \sum_{k=1}^k b_k] \end{aligned}$$

Here  $b_k$  is the data bit of the  $k$ -th user that represents the value either "1" or "0".

$$\left[ \sum_{k=1}^k b_k \right] = [b_1 + b_2 + b_3 + \dots + b_k] = W \quad (15)$$

The photo detector current  $I$  can be represented as:

$$I = I_2 - I_1 = \Re[P_2 - P_1] = \frac{\Re P_r (2W - 2)}{MN - 1} \quad (16)$$

where  $\Re$  is the Responsivity ( $= \eta e / hf$ ) of photo diode.

The aggregate signal power can be represented as:

$$P_s = I^2 = \left[ \frac{\Re P_r (2W - 2)}{MN - 1} \right]^2 \quad (17)$$

The Thermal noise power can be expressed as:

$$P_{ther} = I_{thermal}^2 = \frac{4 K_B T_n B}{R_L} \quad (18)$$

The aggregated shot noise power obtained at photo detectors in the receiver part can be expressed as

$$P_{shot} = I_{shot}^2 = 2eB(I_1 + I_2) = \frac{2eB\Re P_r}{MN-1} \left[ \frac{W^2 + 2W}{2} \right] \quad (19)$$

The total PIIN noise power obtained at photo detectors in the receiver part can be expressed as:

$$\begin{aligned} P_{PIIN} &= I_{PIIN}^2 = BI_1^2 \tau \sum c_k + BI_2^2 \tau \sum c_k \\ &= \frac{B\Re^2 P_r^2 kW}{(MN-1)^2 \Delta v} \left[ \frac{W^2 + 2W}{2} \right] \quad (20) \end{aligned}$$

where

$$\sum c_k = \frac{kW}{MN-1}$$

Since probability of sending either “1” or “0” is 0.5, the  $P_{PIIN}$  can be simplified as:

$$P_{PIIN} = I_{PIIN}^2 = BI_1^2 \tau \sum c_k + BI_2^2 \tau \sum c_k$$

$$= \frac{B\mathfrak{R}^2 P_r^2 kW}{(MN-1)^2 \Delta\nu} \left[ \frac{W^2 + 2W}{4} \right] \quad (21)$$

When a broadband pulse is source input to a group of Fiber Bragg gratings, the incoherent light fields are mixed and applied to the photo detector, and the phase noise of the fields appear in the photo detector output. The coherence time of the thermal source ( $t_c$ ) is expressed as [11]:

$$\tau = \frac{\int_0^\infty G^2(v) dv}{\left[ \int_0^\infty G(v) dv \right]^2} \quad (22)$$

where,  $G(v)$  is the single sideband power spectral density (PSD) of the source.

Taking into consideration aggregate signal power at (17) and various noise powers at (18), (19) and (21), the SNR for the NAND detection technique can be expressed as:

$$SNR = \frac{P_s}{P_{ther} + P_{shot} + P_{PIIN}}$$

$$= \frac{\left[ \frac{\mathfrak{R}P_r(2W-2)}{MN-1} \right]^2}{\frac{4K_B T_n B}{R_L} + \frac{2eB\mathfrak{R}P_r}{MN-1} \left[ \frac{W^2 + 2W}{2} \right] + \frac{B\mathfrak{R}^2 P_r^2 kW}{(MN-1)^2 \Delta\nu} \left[ \frac{W^2 + 2W}{4} \right]} \quad (23)$$

Now using the Gaussian approximation, the bit-error-rate (BER) can be expressed as [12]:

$$BER = P_e = \frac{1}{2} \operatorname{erfc} \left( \sqrt{\frac{SNR}{8}} \right) \quad (24)$$

### V. NETWORK SIMULATION SETUP

The simulation set up for OCDMA system based on 3-D MQC/MP code using NAND subtraction technique consisting three users, is implemented using simulation software Opti-system version 12.0 consist of transmitter, receiver and single mode fiber.

As presented in Fig. 1, the transmitter circuit contains Continuous Wave Laser Array, power splitter, encoder circuit and power combiner. The Encoder consists of three sets of Optical Filters implemented using fiber Bragg gratings (FBG) and Time Delay circuits. The broad band light source is sliced using splitter produces sliced chips having spectral width of 0.1 nm modulated by pseudo random bit sequence (PRBS).

The CW laser array is used for generating light pulses. The wavelengths range from 193.1 nm to 193.8 nm, with 0.1 nm wavelength spacing. Eight CW lasers (wavelength 1-8) are used to create a dense WDM multi-frequency light source i.e. carrier signal using WDM Multiplexer. The generated carrier is used to modulate the pseudo-random bit sequence data of user. The data rate used in the system is 2.5 Gbps and the input power is 10dBm The NRZ pulse generator is used to convert logical data into electrical signal. A Mach-Zehnder modulator which is an external modulator is using On-Off keying to modulate the multiplexed eight wavelengths according to NRZ electrical data. The modulated signals are distributed to the respective encoders using power splitter, which have been assigned a unique MQC/MP code respective to each encoder. The encoded data from all the users are multiplexed by power combiner and then passed through 0.5-50 km single mode optical fiber followed by a loss compensating Optical Amplifier with gain 10 dB and noise figure of 4dB. The structure of the Receiver is shown in Fig. 2 composed of MUX, DEMUX, six sets of PIN Photo Detectors (PDs), Low Pass Filters, Regenerators, NAND subtractors and Eye diagram Analyzers. The Decoder consists of six sets of Optical Filters and Inverse Time Delay (ITD) circuits.

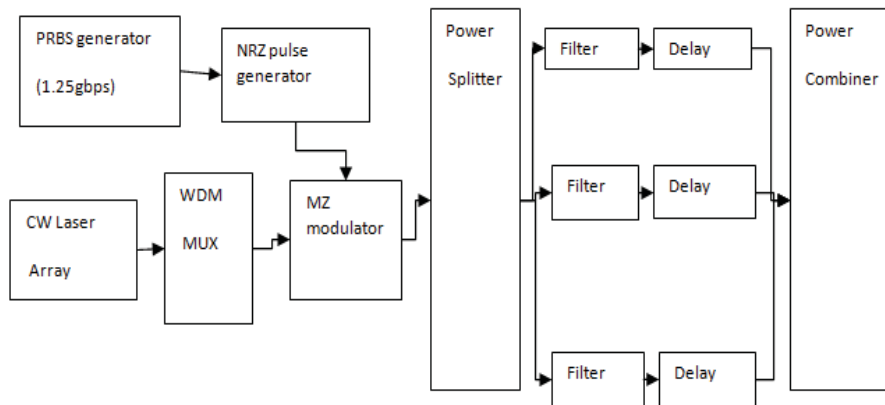


Fig. 1 Transmitter of 3-D MQC/MP OCDMA Network

The received data from the transmitter are amplified and demultiplexed at the beginning of the receiver. The demultiplexed data is decoded by the sets of Optical Filters and ITD circuits. The six sets of PIN Photo Detectors (PD) are used to convert optical data to electrical signal which is then transmitted through a low pass Bessel Filter and regenerators. Eyediagram analysers are connected at the end to analyse the received signal. The generated noise at the receiver side is random in nature and un-correlated. The system performance is estimated by referring to SNR and BER.

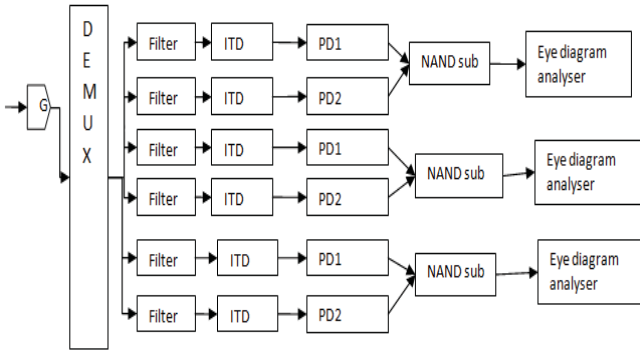


Fig. 2 Receiver of 2-D MQC/MP OCDMA Network

## VI. SIMULATION RESULTS

In this part of the paper, we have evaluated the performance based on theoretical analysis and simulation results according to the typical system parameters, as listed in Table VI.

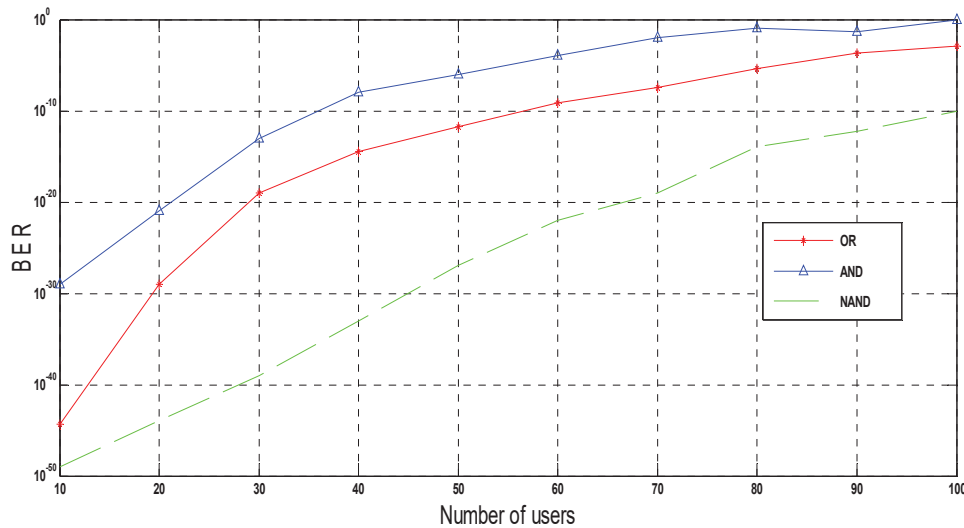


Fig. 3 BER vs number of active users

| Sl. no | Parameters           | Quantity           |
|--------|----------------------|--------------------|
| 1      | Line encoder         | NRZ                |
| 2      | Effective power      | 0 to -10 dBm       |
| 3      | No of users          | 10 to 200          |
| 4      | Operating wavelength | 1550 nm            |
| 5      | Fibre length         | 10 to 50 km        |
| 6      | Data rate            | 622 mbps to 1 gbps |
| 7      | Received power       | 0 to -35 dBm       |
| 8      | Fibre attenuation    | 0.2 dB/km          |
| 9      | Dispersion           | 16.75 ps/nm/km     |
| 10     | PMD coefficient      | 0.5 ps/sqrt (km)   |

The bit-error-rate (BER) performance of 3-D MQC/MP code using AND, OR and NAND subtraction technique for various numbers of active users is shown in Fig 3.

It can be seen from Fig. 3 that the NAND subtraction technique is much more effective in reducing the MAI and BER than other detection techniques. Also the BER level is lower for higher number of users in NAND detection technique employed for 3-D MQC/MP code.

Fig. 4 shows the SNR versus the number of active users. It can be observed that the 3-D MQC/MP codes provide much better SNR values using NAND detection technique compared to OR and AND detection techniques for higher effective power.

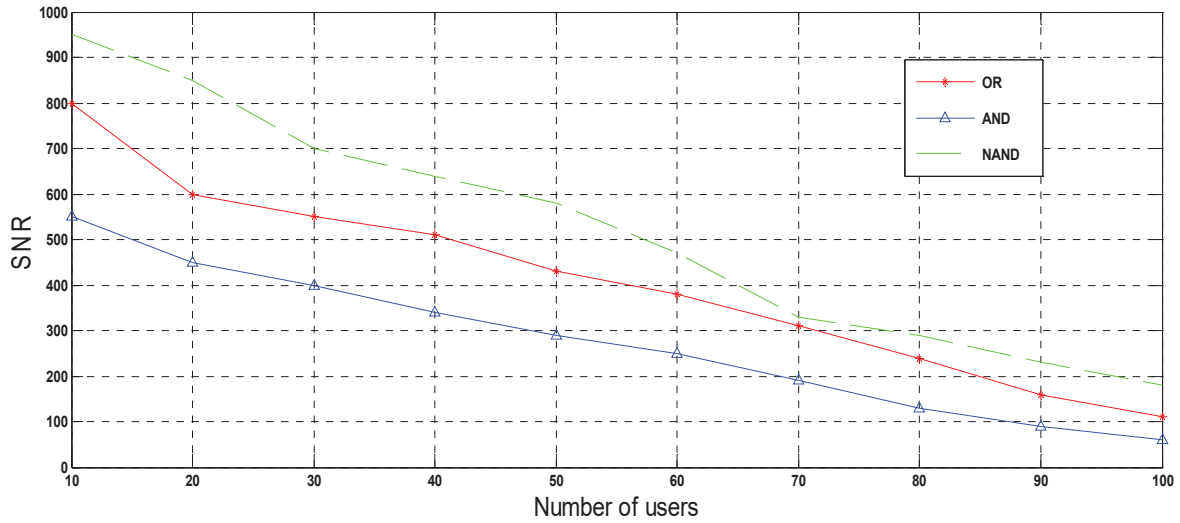


Fig. 4 SNR vs number of active users

The eye diagrams of the received signals for various detection techniques are shown in Figs. 5 (a)-(c). It can be observed that the system produces higher signal quality with NAND detection technique compared to other detection

techniques like AND and OR for 3-D MQC/MP codes. The more the eye closes, difficulty arises in identifying ones and zeroes in the signal. The height of the eye opening at a certain time represents the noise immunity of the signal.

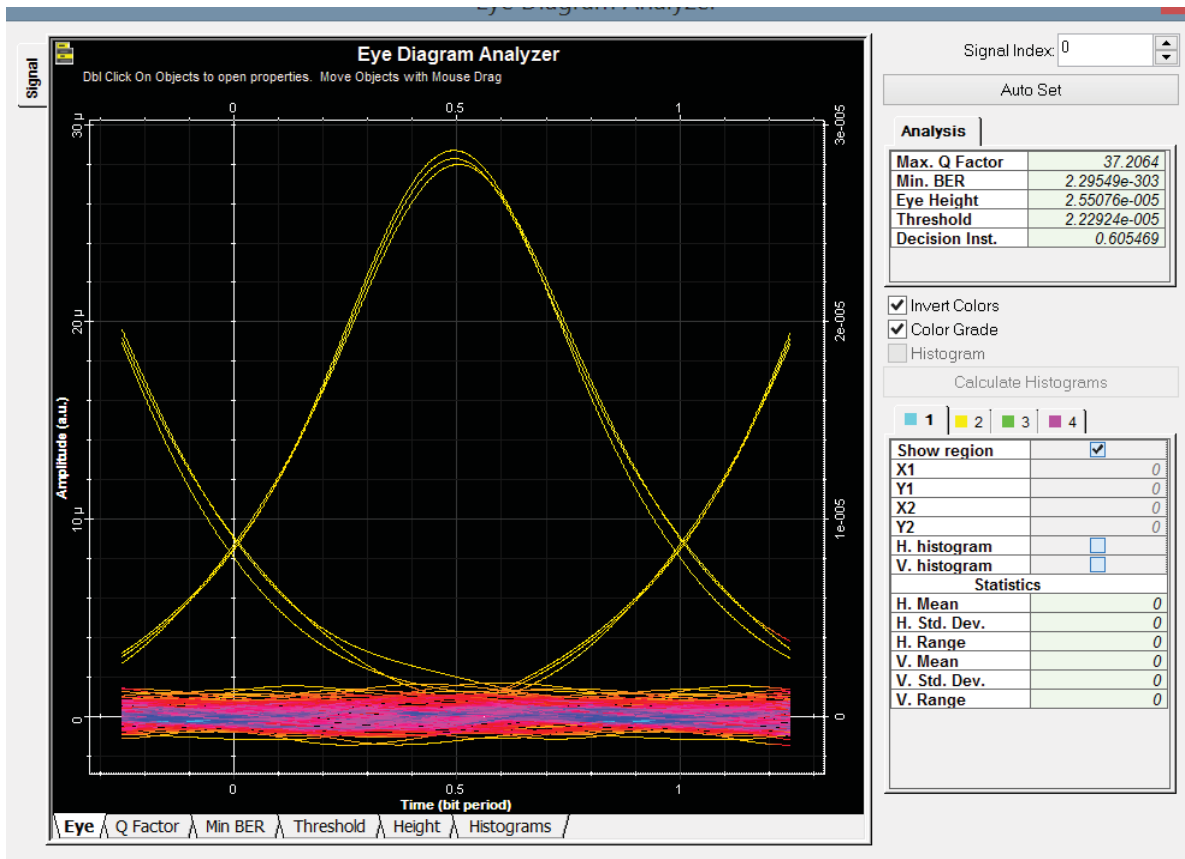


Fig. 5 (a) Eye diagram at 622 Mbps for NAND detection technique in receiver

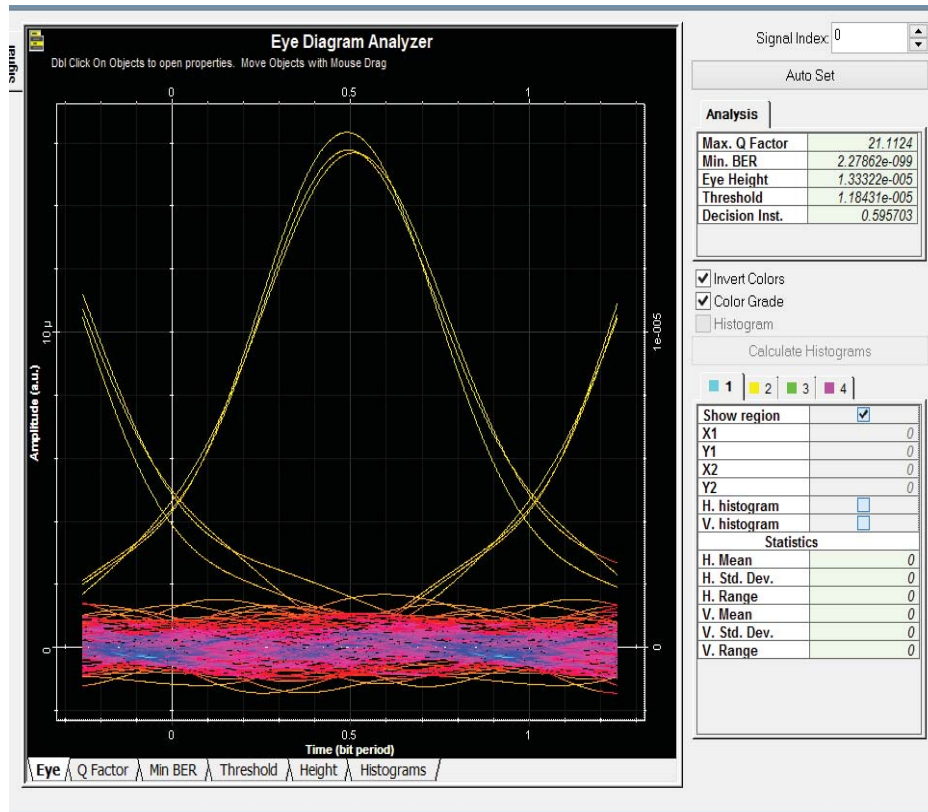


Fig. 5 (b) Eye diagram at 622 Mbps for OR detection technique in receiver

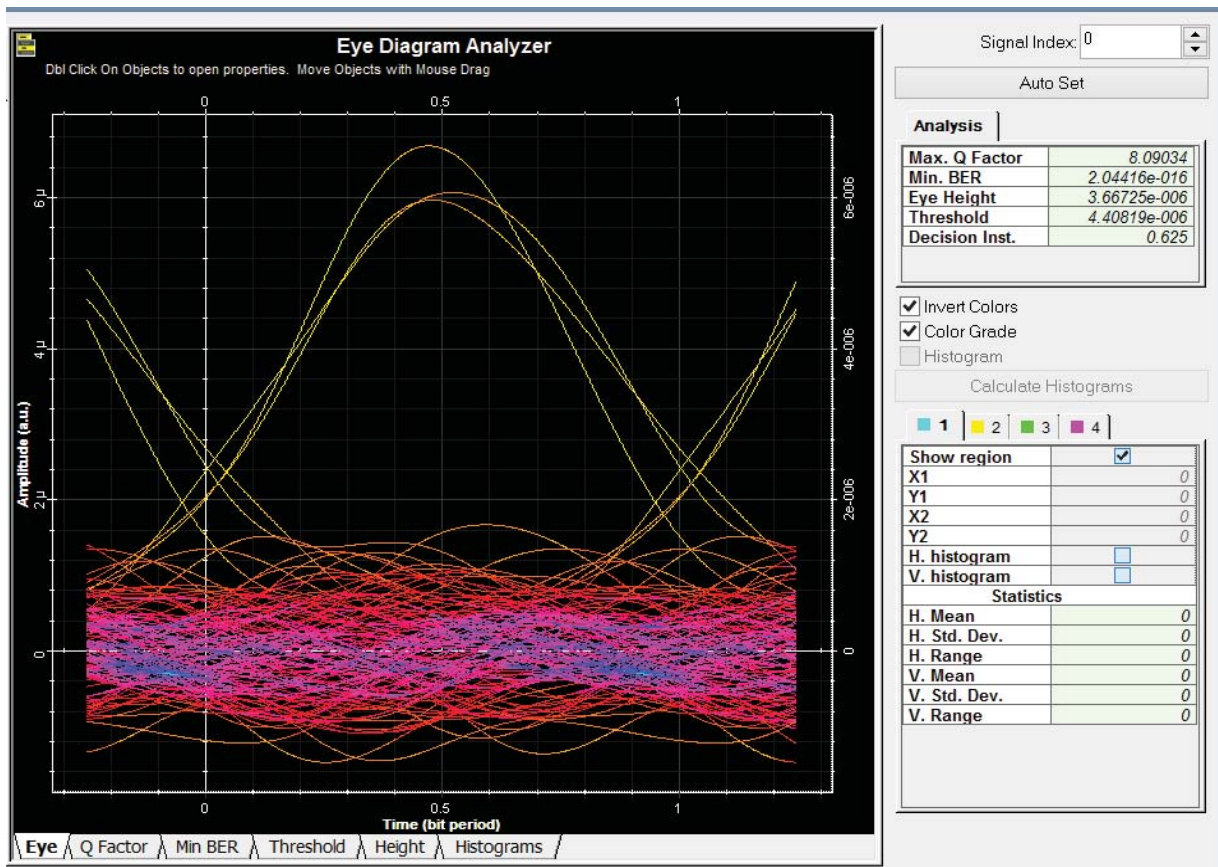


Fig. 5 (c) Eye diagram at 622 Mbps for AND detection technique in receiver



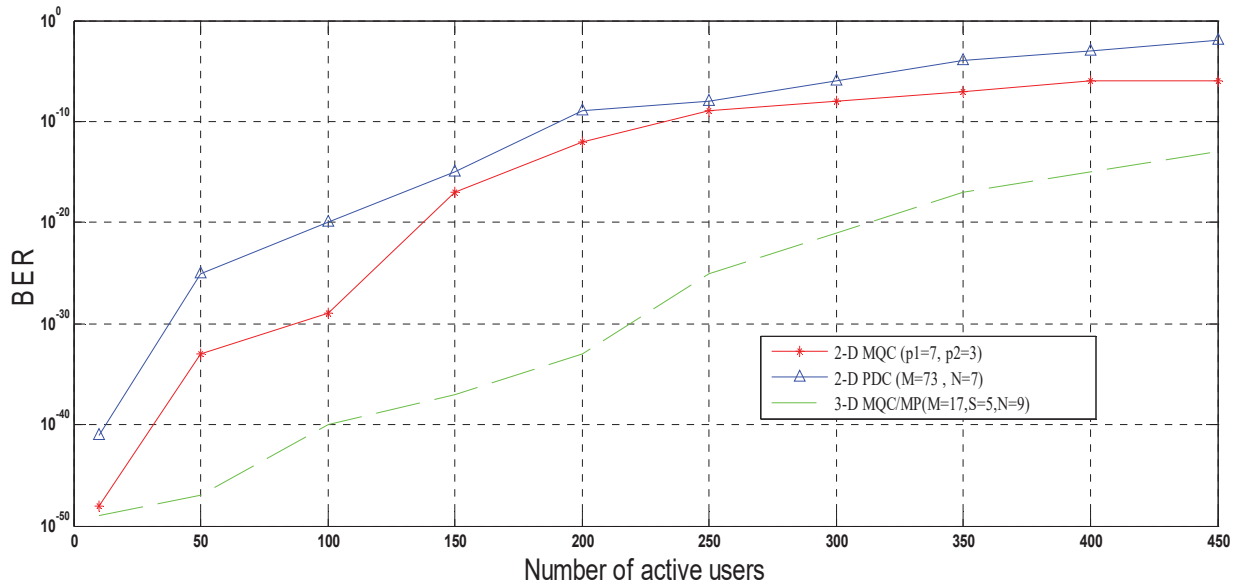


Fig. 6 BER vs number of active users for various types of 3-D codes

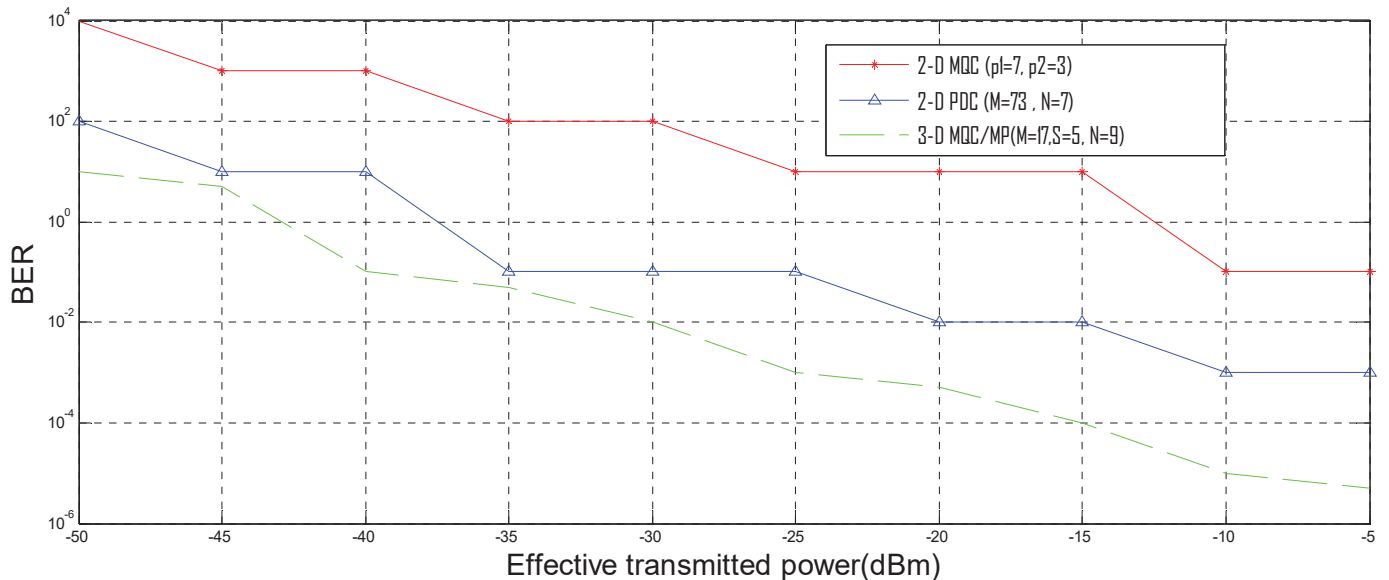


Fig. 7 BER vs Effective transmitted power (dBm) for various types of codes

The BER variation against number of simultaneous users for different types of 3-D and 2-D codes is demonstrated in Fig. 6. It can be observed that BER performance is much better for 3-D MQC/MP code in comparison to 2-D perfect difference (PDC) [13] code and 2-D MQC code for a given number of simultaneous users.

The BER variation against effective transmitted power (dBm) for various types of 3-D codes is demonstrated in Fig. 7. It can be observed that the proposed 3-D MQC/MP code requires lowest optical transmission power compared to other codes like 2-D MQC and 2-D PDC codes because of effective suppression of PIIN noise.

## VII. CONCLUSION

In this paper, we have proposed a new 3-D MQC/MP optical CDMA code for enhancing system performance by suppressing various types of noises like thermal noise, shot noise and PIIN noise. The system architecture of the 3-D code is also explained in detail which achieves higher cardinality, better BER performance and lower effective transmitted power compared to other two dimensional OCDMA codes. The performance degradation due to PIIN noise can be minimized by lowering cross-correlation and BER [14]. We have also analyzed the OCDMA system performance for 3-D MQC/MP code for three different detection techniques like NAND, OR and AND subtraction techniques. The analysis result obtained by the NAND detection technique with 3-D MQC/MP code found to be supporting more number of

simultaneous users and it can improve the system performance by minimizing the MAI significantly in comparison to other detection techniques like the OR and AND subtraction technique.

#### ACKNOWLEDGMENT

The authors would like to extend their sincere appreciation to the All India Council of Technical Education (AICTE) for the funding of this research through the research project number 20/AICTE/RIFD/RPS (POLICY-II) 2/2012-13.

#### REFERENCES

- [1] Zouine Y, Dayoub I, Haxha S and Rouvaen J. M., "Analyses of constraints on high speed optical code division multiplexing access (OCDMA) link parameters due to fiber optic chromatic dispersion", *Journal of Optical Communication*. vol. 281, 2008, pp. 1030–1036.
- [2] Santoro M A and Fan T R., "Spread spectrum fiber optic local area network using optical processing", *Journal of Light wave Technology*. vol. 4, 1986, pp.547–554.
- [3] Zou Wei, H.M.H Shalaby, H Ghafouri-shiraz, "Modified quadratic congruence code for fiber Bragg Grating based spectral amplitude coding optical CDMA system". *Journal of light wave technology*. vol 19, 2001, pp.1274-1281.
- [4] Yang G.C and Kwong W.C., "Prime code with applications to CDMA optical and wireless networks", *Boston: Artech House*, 2002.
- [5] Hasson F N, Aljunid S A, Samad M.D.A and Abdullah M K., "Spectral amplitude coding OCDMA using AND subtraction technique", *Application of Optics*. vol. 47, 2008, pp. 1263–1268.
- [6] M.K. Abdullah, N.F. Hasoon, S.A. Aljunaid, S. Shaari., "Performance of OCDMA systems with new spectral direct detection (SDD) technique using enhanced double weight (EDW) code", *J. Opt. Communication*, vol.281, 2008, 4658-4662.
- [7] N. Ahmed, S.A. Aljunaid, A. Fadil, R.B. Ahmad, M.A. Rashid., "Performance enhancement of OCDMA system using NAND detection with modified double weight (MDW) code for optical access network", *Journal of Optik*, vol.124, 2013, pp.1402-1407.
- [8] Mohammed Noshad, and Kambiz Jamshidi., "Code family for modified spectral amplitude coding OCDMA system and performance analysis", *Journal of Optical Communication Networks*. vol. 2, 2010, pp. 344–354.
- [9] Aljunaid S.A, Ismail M, and Ramil A.R., "A new family of optical code sequence for spectral-amplitude-coding optical CDMA systems", *IEEE Photonic Technology Letters*, vol. 16, 2004, pp. 2383–2385.
- [10] M.S Anwar, S.A. Aljunaid, N.M. Saad, S.M. Hamzah, "New design of spectral amplitude coding in ocdma with zero cross correlation", *Journal of optical communication*, vol.282,2009,pp.2659-2664.
- [11] H.A. Fadhil, S.A. Aljunaid, H.Y. Ahmed, H.M.R. Alkhafaji, "Variable cross-correlation code construction for spectral amplitude coding optical CDMA networks". *Journal of Optik*, vol.123, 2012, pp.956-963.
- [12] M H Kakaee, Saleh S,H A Fadhil, S B A Anas, M Mokhtar. "Development of Multi-Service (MS) for SAC-OCDMA system". *Journal of Optic & Laser technology*.vol.60, 2014, pp.49-55.
- [13] J.H. Wen, J.S. Zhou, C.P. Li, "optical spectral amplitude coding CDMA systems using perfect difference code and interference estimation", *IEEE proceedings Optoelectronics*, vol.153, 2006, pp.152-160.
- [14] Z. Wei, H. Ghafouri-Shiraz. "Codes for spectral-amplitude-coding optical CDMA systems", *J. Lightwave Technol*, vol.20, no.8, 2002, pp.1284–1289.